THE DEVELOPMENT AND TEST OF

MULTI-ANODE MICROCHANNEL ARRAY DETECTOR SYSTEMS

II.   SOFT X-RAY DETECTORS

J. G. Timothy
Principal Investigator

Center for Space Science and Astrophysics
Stanford University
Stanford, California 94305-4055

During the past six months a number of significant evaluations were undertaken as part of this development program. In particular, the initial scrub and evaluation of the curved channel microchannel plate (MCP) was completed, the first images at soft x-ray wavelengths (8 keV) were recorded with the (256 x 1024)-pixel MAMA detector on the SPEAR storage ring at the Stanford Synchrotron Radiation Laboratory (SSRL), and the initial evaluations of the first two "off-axis channel" macroplates were completed.

The results with the curved channel MCP with the curved front face and the planar output face were most encouraging. Gain saturation was obtained over the entire active area even though the 250 mm radius-of-curvature of the front face resulted in a change in the channel length-to-diameter ratio from the center to the edge from about 106:1 to about 136:1. This is in marked contrast to the failure of other investigators to operate a "chevron" MCP with a curved front face and a planar output face. At an applied potential of 1950 V the resolution of the output pulse-height distribution was 40% at the center and 79% at the edge of the MCP. The evaluation of this MCP is continuing.

Imaging tests of the (256 x 1024)-pixel MAMA detectors at ultraviolet and visible wavelengths have demonstrated the theoretical spatial resolution of 25 microns and the ability to locate the centroid of a spatial or spectral feature to an accuracy of better than 1 micron. The initial imaging tests at soft x-ray wavelengths have been carried out on the x-ray diffraction beam line at SSRL at an energy of ∿8 keV. A diffraction pattern of a protein crystal recorded with a demountable (256 x 1024)-pixel MAMA detector with a Be window is shown in Figure 1. Preliminary analysis of these data indicate that the MAMA is again yielding a theoretical response of 25 microns. Further detailed analyses of these data are now in progress.

Figure 1.   Part of an x-ray diffraction pattern from a protein crystal.
Scattering of x-rays from the beam stop can be seen at the center of the image.

The initial evaluations of the totally new type of high-gain MCP, the "off-axis channel" MCP fabricated by Detector Technology Inc. (Detech) are highly encouraging. The "off-axis channel" macroplate with channel diameters of 75 microns and channel length-to-diameter ratios of 60:1 yielded a modal gain of 2.6×10^6 electrons pulse-1 and a resolution of the output pulse-height distribution of 64% at an applied potential of 2400 V. Details of these tests are given in the preprint attached to this report.

Under this grant we have recently ordered from Detech two "off-axis channel" MCPs with 50-micron channel diameters and four channels per single fiber element to increase the open area ratio.

The design of the demountable detector tube with the attached residual gas analyzer (RGA) has been completed and we are now ready to start CsI photocathode processings at EMR Photoelectric Inc.

We have requested a 90 day no-cost extension to the grant in order to permit first, the completion of the initial evaluations of the "off-axis channel" MCPs and, second, to allow time for the submission and review of a proposal for a 24 month funded continuation of this grant. The goal is to verify the imaging capabilities of the MAMA detectors at soft x-ray wavelengths using the SSRL facilities and to validate the "off-axis channel" MCP concept in the high resolution format (channel diameters of the order of 10 to 12 microns).

Attachments

"Imaging at Soft X-ray Wavelengths with High-Gain Microchannel Plate
Detector Systems," by J. G. Timothy. To appear in SPIE X-ray Imaging
II, 1986.

"The Off-axis Channel Macroplate," by J. G. Timothy. To appear in SPIE
Ultraviolet Technology, 1986.

MULTI-ANODE MICROCHANNEL ARRAY

four-fold coincidence-anode array

FEEDBACK-FREE
MICROCHANNEL PLATE

COINCIDENCE-ANODE
ARRAY

UPPER PLANE
CODING ELECTRODES

OPAQUE PHOTOCATHODE

INPUT-FACE ELECTRODE
(~-2000 V)

FEEDBACK-FREE MCP
(C-PLATE)

QUARTZ SUBSTRATE

OUTPUT-FACE ELECTRODE
(0 V)

LOWER PLANE
CODING ELECTRODES

SiO_2 INSULATING LAYER

OUTPUT CHARGE PACKET (~10^6 electrons per pulse)

UPPER PLANE
CODING ELECTRODES
(~75 V)

LOWER PLANE CODING ELECTRODES (~75 V)

QUARTZ SUBSTRATE

Figure 1.   Schematic of an imaging MAMA detector tube with a multi-layer
            coincidence-anode readout array.

Focus Electrode

Opaque Photocathode
on Funneled Channels

Curved-Channel MCP

Anode Array

$h\nu$

Thin Film XUV Filter

Low Density CsI
Photocathode

50 Å Thick SiO_2
Ion Barrier Membrane

Curved-Channel MCP

Anode Array

(a)   (b)
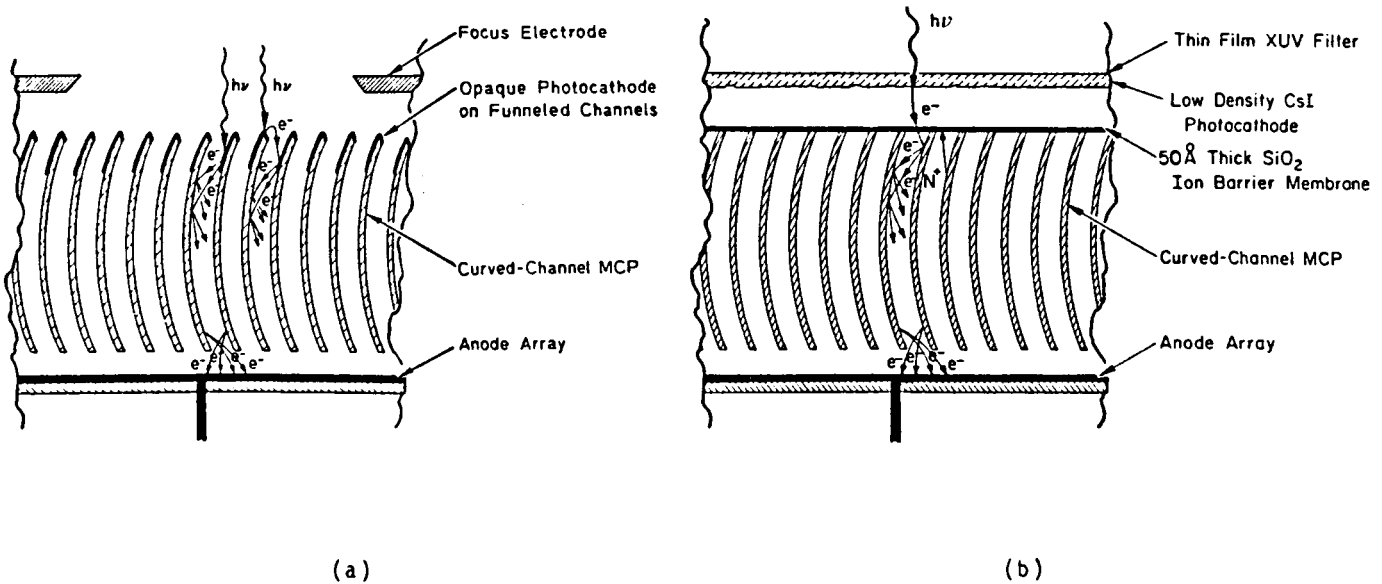
Figure 2.   Configurations of CsI photocathodes for use at extreme-ultraviolet
            (EUV) and soft x-ray wavelengths.

        a. High-density (opaque) CsI deposited on the front surface of the MCP.
        b. Low-density (fluffy) CsI mounted in proximity focus with the
            front face of the MCP.

The way in which the coincidence-detection technique operates is shown in Fig. 3. In the one-dimensional array shown in Fig. 3a, a charge pulse detected on a fine-position-encoding electrode can have originated from any one of sixteen pixel electrodes in the active area of the array. This ambiguity is removed by interlaced sets of coarse-position-encoding electrodes. There is only one position along the array where a particular fine-encoding electrode and a particular coarse-encoding electrode are adjacent. The coincident arrival of charge pulses on a fine and a coarse electrode accordingly uniquely defines in one dimension the location of the detected photon event. Using this technique, a x b pixels can be identified with only a + b amplifier and discriminator circuits. In the configuration shown in Fig. 3a, for example, 1024 pixels can be uniquely identified with only 64 amplifier and discriminator circuits. Two-dimensional imaging arrays are fabricated by producing a multilayer structure in which two coincidence-anode arrays are laid out othogonally on top of each other. The configuration of a (1024 x 1024)-pixel array, which requires only a total of 128 amplifier and discriminator circuits, is shown in Fig. 3b.

(a)   (b)
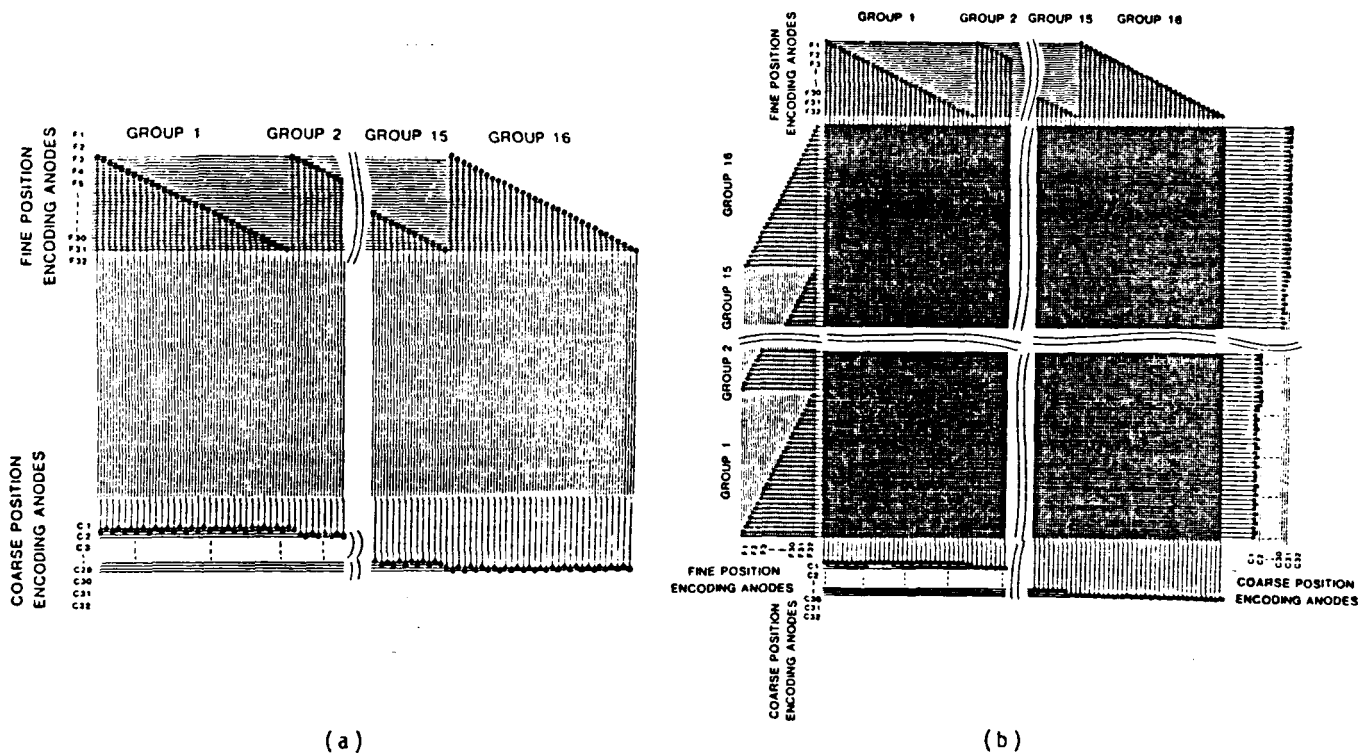
Figure 3.   Schematics of coincidence-anode readout arrays.

a.   One-dimensional (1 x 1024)-pixel array.
b.   Imaging (1024 x 1024)-pixel array.

A technical problem with the fabrication of these arrays is associated with the fact that the energy of the output electrons from the MCP is very low (~30 eV). The electrons are accordingly unable to penetrate any insulating layer. This problem is overcome during the fabrication process by etching away the insulating dielectric in the interstices between the upper layer electrodes. This allows part of the charge cloud to pass directly to the lower electrodes. In the present generation of MAMA detectors, which have pixel dimensions of 25 x 25 microns^2, curved-channel MCPs with 12-micron-diameter channels on 15-micron centers are employed in order to guarantee good uniformity of response and ensure that there are no moiré patterns in the flat-field response caused by the pitch of the channels beating against the pitch of the anode structure. In practice, it is not possible to exactly align the grid of electrodes with the channels which are packed in a hexagonal configuration. In addition, the single high-gain curved-channel MCP is operated in the space charge saturated mode and, as shown in Fig. 4a, the charge cloud from the channel spreads apart rapidly under the effects of space-charge repulsion. With an MCP-to-anode-array spacing of the order of 50 microns and an accelerating potential on the anode array of about 100 V the output charge cloud from the 12-micron-diameter channel will spread to a diameter of about 30 to 40 microns. The address-decoding circuits in the MAMA electronics have accordingly been programmed to detect coincident pulses on two or three adjacent electrodes, as shown in Fig. 4b. In this way positional information is obtained in 12.5-micron spatial bins in each axis of the array.
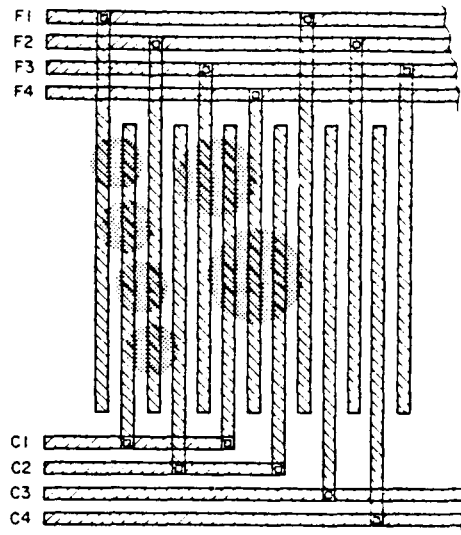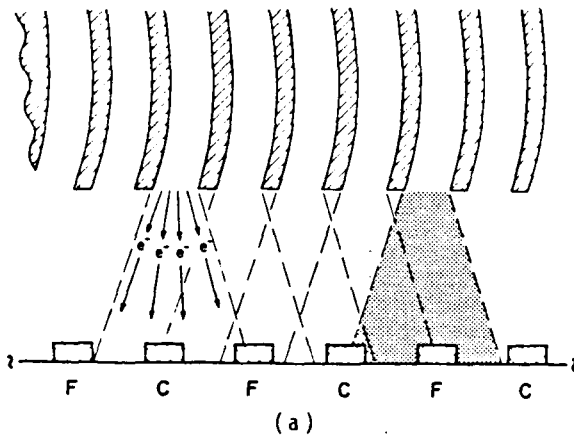
Figure 4. Position-encoding scheme
employed in the present
generation of MAMA detectors.

a. Schematic showing the expansion
of the charge cloud from the MCP
under the effects of space-charge
repulsion.

b. Schematic showing the relative
sizes of the charge cloud for
allowed and rejected events. All
events which stimulate more than
three adjacent electrodes are rejected
in the present generation of arrays.

ALLOWED: F1 + C1   2 FOLD
          F1 + C1 + F2   3 FOLD
          C1 + F2   2 FOLD
          C1 + F2 + C2   3 FOLD
          etc.

REJECTED: C2 + F3 + C1 + F4   4 FOLD
           etc.
           F3 + C2 + F4 + C2 + F1   5 FOLD
           etc.

(b)

Adjacent bins of two-fold and three-fold events in each axis are added to produce the
25-micron-wide pixel. Events occurring on four or more electrodes in each axis
simultaneously, or on non-adjacent electrodes, are rejected. This guarantees that there is
no degradation of the image quality at high count rates when the possibility for the
simultaneous arrival of photon events increases to a significant level.

The imaging array which is being used for the evaluation and optimization of the MAMA
detector systems at this time is the (256 x 1024)-pixel array with pixel dimensions of
25 x 25 microns^2 and an active area of 6 x 26 mm^2 (see Fig. 5) which can be accommodated
within the active area of a 25-mm-format curved-channel MCP.
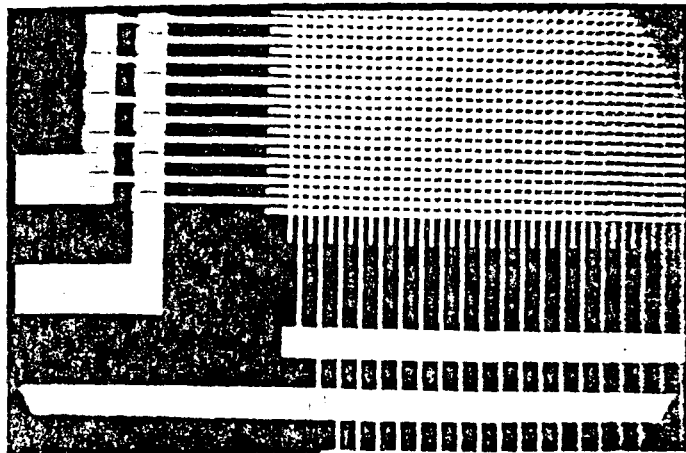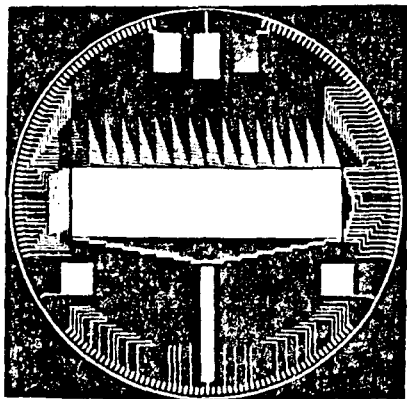
(a)

(b)

Figure 5. (256 x 1024)-pixel coincidence-anode array with 25 x 25 microns^2 pixels.

a. Array fabricated on a 38-mm-diameter substrate.
b. Magnified view of a corner of the active area showing the multi-layer electrode
structure. The pixel electrodes have a 25-micron center-to-center spacing.

Performance Characteristics

Since the event-detection technique employs high-speed digital electronics, the output count rate from the MAMA detector is essentially determined by a speed and power trade-off in the electronics. The pulse-pair resolution of the existing second-generation MAMA electronics is 100 ns and the variation of the DQE as a function of count rate has the form shown in Fig. 6. A 10% loss of DQE is obtained with this system at 10^6 counts s^{-1} (random) from each array. The existing electronics technology can provide an ultimate pulse-pair resolution in the range from 20 to 50 ns at the cost of increased power consumption if a higher count rate capability is required for a particular application. It should also be noted that the address of the detected event is automatically generated in the electronic circuits. The MAMA is accordingly a random readout detector which can identify the arrival time of the detected photon to an accuracy comparable to the resolution time of the address-decoding circuits. This gives the MAMA a unique event-timing capability and images can be recorded in two ways. First, the digital image can be integrated in a random access memory, and, second, the address coordinates and arrival times of each detected photon can be stored in real time on a recording medium such as magnetic tape.[6]
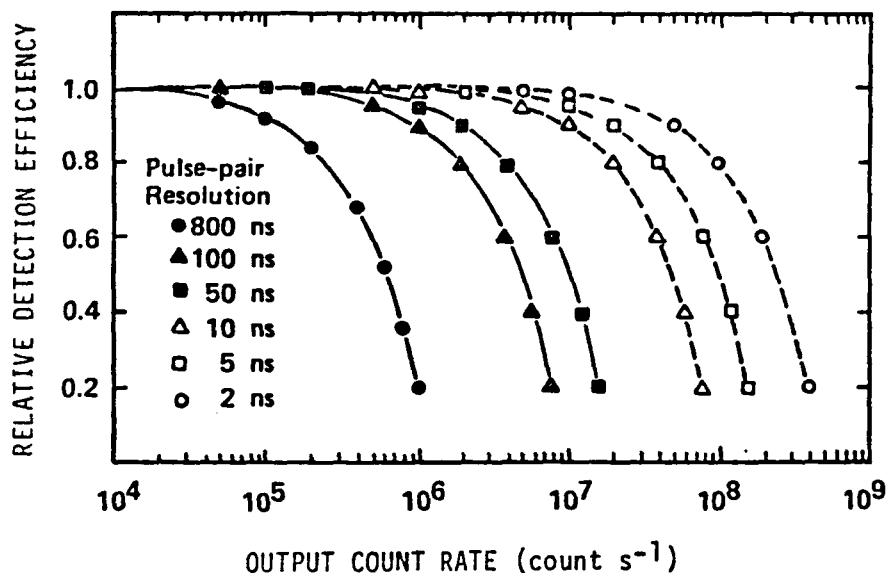
Figure 6. Variation of the detection efficiency as a function of output count rate for MAMA detector systems with different pulse-pair resolutions. The existing electronics technology can provide an ultimate pulse-pair resolution in the range from 20 to 50 ns.

When properly conditioned by the appropriate bake and burn-in procedures, the curved-channel MCPs operate with a highly uniform response, excellent gain stability and very narrow output pulse-height distributions.[2] Lifetimes in excess of 2.5×10^{11} counts mm^{-2} have already been demonstrated at ultraviolet wavelengths. Measurements at soft x-ray wavelengths show that there is a significant increase in the gain with increasing photon energy at wavelengths below 100 Å. A gain increase of 30% has been observed for a bare MCP at a wavelength of 1.5 Å when compared with data taken at ultraviolet wavelengths. This effect is much stronger for a CsI-coated MCP and can be used to provide coarse energy discrimination at soft x-ray wavelengths.[7]

The curved-channel MCPs currently being used have exhibited a 10% loss of DQE at count rates of the order of 100 counts s^{-1} (random) for each 25 x 25 microns^2 pixel. The first curved-channel MCPs fabricated with the new high-conductivity "Long-Life" (L^2) glass have just been received and can be expected to improve this count rate capability by at least a factor of five. MAMA detectors have already been operated successfully at EUV wavelengths with CsI coatings deposited on the front-face. A quantum efficiency as high as 40% has been obtained at 1216 Å for such a configuration where the CsI was deposited and preserved at all times under vacuum.[8] The dark count rate for this detector is of the order of 0.1 counts mm^{-2} s^{-1}. A demountable MAMA detector with a high-vacuum gatevalve has recently been constructed for studies of CsI in both high- and low-density configurations at soft x-ray wavelengths.

Imaging tests at ultraviolet wavelengths have verified that the MAMAs are obtaining the theoretical resolution of 25 microns FWHM.[9] Recent laboratory measurements have also shown that the centroid of a spectral feature can be determined to an accuracy of the order of 1 micron. Initial imaging tests at a wavelength of 1.5 Å on the storage ring at the Stanford Synchrotron Radiation Laboratory (SSRL) indicate that the imaging performance is not degraded at soft x-ray wavelengths. More detailed evaluations at soft x-ray wavelengths will be undertaken during the coming year.

Future Developments

A number of improvements to the key components of the MAMA detectors are currently being implemented. These include the use of high-speed, high-input-capacitance amplifiers and high-conductivity curved-channel MCPs with 10-micron-diameter channels to further increase the maximum count-rate capability and to improve the uniformity of response of the imaging systems, and new anode-array geometries to further increase the DQE. The optimized (256 x 1024)-pixel detector system is expected to be in operation later this year. The achieved performance characteristics and the performance goals for the systems to be fabricated during the next three years of the development program are given in Table 1.

Table 1. MAMA Detector System Performance Characteristics

	Achieved	Goal
MCP active area	75 mm diameter	150 mm diameter
Anode array format	256 x 1024	1024 x 1024 2048 x 2048 4096 x 4096
Spatial resolution	25 μm (FWHM) (rate-independent)	18 μm (FWHM) (later 12 to 14 μm (FWHM)) (rate-independent)
Position sensitivity for centroiding	$\sim$ 1 μm	< 1 μm (signal-to-noise dependent)
Wavelength range	1150 to 8500 Å (sealed) 1.5 to 1400 Å (open)	1150 to 9500 Å (sealed) $\sim$ 1 to 1400 Å (open)
Peak quantum efficiency	15 to 20% ultraviolet and visible 40% far ultraviolet	> 30% ultraviolet and visible > 50% EUV > 20% soft x-ray
Pulse-counting detective quantum efficiency	65 to 80% of Q.E.	> 85% of Q.E.
Flat-field uniformity	< 25% peak-to-peak	< 5% peak-to-peak
Defect levels: anode array MCP bright spots MCP dark spots	 zero zero 5 to 10	 zero zero < 5
Spatial linearity	± 5 μm over 26 mm	± 5 μm over 90 mm
Maximum count rate (10% loss of DQE) per pixel (25 x 25 μm^2) per array	 $\sim$ 100 counts s^{-1} (random) 10^6 counts s^{-1} (random)	 > 1000 counts s^{-1} (random) > 10^7 counts s^{-1} (random)
Lifetime	> 2.5 x 10^{11} counts mm^{-2} (25-μm-pore-size MCP at 10^6 gain)	> 10^{13} counts mm^{-2}
Operating temperature range	+30 to -30 °C	+30 to -30 °C
Total system power (does not include cooling)	< 30 W (speed dependent)	< 60 W (speed dependent)

In parallel with the continuing optimization program, the fabrication of the (1024 x 1024)-pixel array with 25 x 25 microns^2 pixels, which requires a 40-mm-format high-gain MCP, has been initiated, and the fabrication of the STIS (2048 x 2048)-pixel array with 25 x 25 microns^2 pixels, which requires a 75-mm-format high-gain MCP, will be initiated later this year. The goal is to have the (1024 x 1024)-pixel detector in operation by the summer of 1987 and the (2048 x 2048)-pixel detector in operation by the spring of 1988.

The STIS detector is constructed from four independent (1024 x 1024)-pixel arrays fabricated on a single substrate with a single pixel deadspace between adjacent arrays, as shown in Fig. 7. This will significantly increase the dynamic range of the detector and will provide the redundancy required for a long-duration space mission.
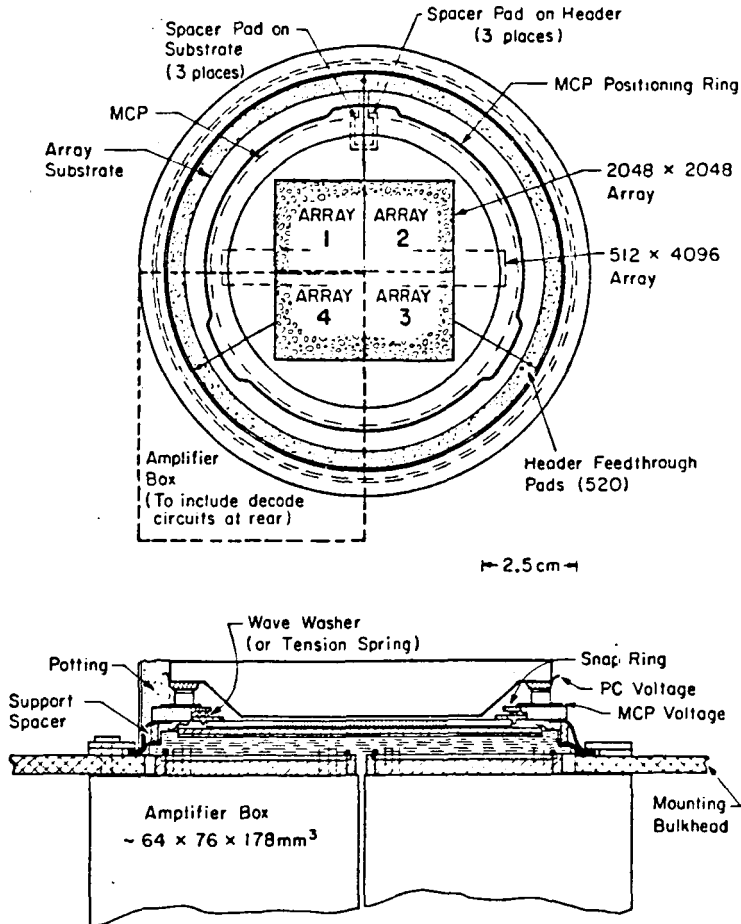
Figure 7. Configuration of the (2048 x 2048)-pixel MAMA detector for the
Hubble Space Telescope Imaging Spectrograph (STIS).

The equipment that will be used to fabricate the anode arrays for STIS will be able to accommodate substrates with diameters of up to about 150 mm in diameter. It will, therefore, be possible to use the basic technology of the STIS detector to fabricate ultra-large-format arrays. As an example of one of the possible configurations that could be constructed, the schematic of a (1024 x 1024)-pixel array with pixel dimensions of 80×80 microns^2 that could be used as a detector for soft x-ray diffraction studies is shown in Fig. 8. If the STIS detector program proceeds at the expected rate, detector systems of this size could be available within three years.

Acknowledgements
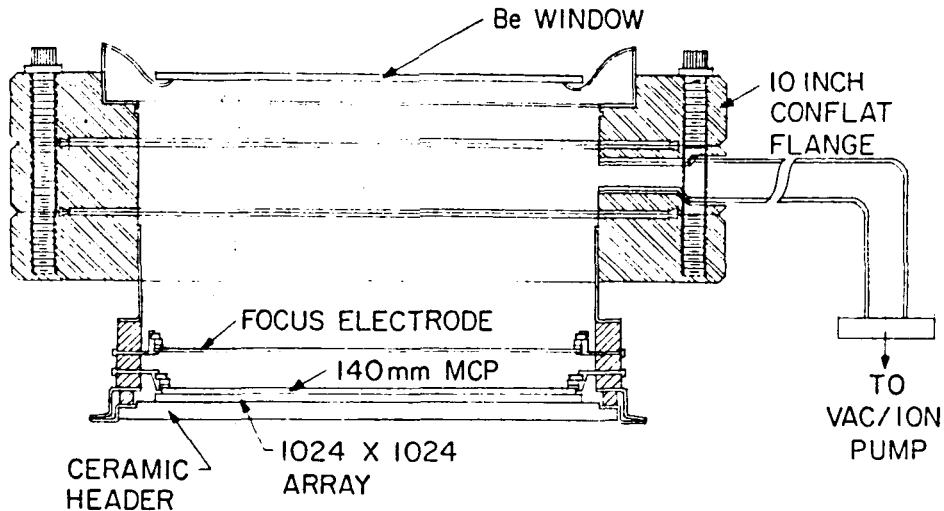
Figure 8. Schematic of an ultra-large-format soft x-ray MAMA detector with an array active area of 80 x 80 mm^2.

References

1. Timothy, J. G., "Optical Detectors for Spectroscopy," Publications Astron. Soc. Pacific 95, 810. 1983.

2. Timothy, J. G., "Multi-Anode Microchannel Array Detector Systems: Performance Characteristics," Optical Engineering 24, 1066. 1985.

3. Timothy, J. G., "Electronic Readout Systems for Microchannel Plates," IEEE Transactions on Nuclear Science NS-32, 427. 1985.

4. Woodgate, B. E. and the Space Telescope Imaging Spectrograph Science Team, "Second-generation Spectrograph for the Hubble Space Telescope," to appear in SPIE Instrumentation in Astronomy VI, 1986.

5. Bateman, J. E. and R. J. Apsimon, "A New Photocathode for X-ray Image Intensifiers Operating in the 1-50 KeV Region," Advances in Electronics and Electron Physics 52, 189. 1979.

6. Timothy, J. G. and J.S. Morgan, "Imaging by Time-Tagging Photons with the Multi-Anode Microchannel Array Detector System," to appear in SPIE Instrumentation in Astronomy VI, 1986.

7. Fraser, G. W. and J. F. Pearson, "Soft X-ray Energy Resolution with Microchannel Plate Detectors of High Quantum Detection Efficiency," Nuclear Instruments and Methods 219, 199. 1984.

8. Timothy, J. G., G. H. Mount and R. L. Bybee, "Multi-Anode Microchannel Arrays," IEEE Transactions on Nuclear Science NS-28, 689. 1981.

9. Timothy, J. G. and R. L. Bybee, "High-Resolution Pulse-Counting Array Detectors for Imaging and Spectroscopy at Ultraviolet Wavelengths," to appear in SPIE Ultraviolet Technology. 1986.

The off-axis channel macroplate

J. Gethyn Timothy

Center for Space Science and Astrophysics, Stanford University,
ERL 314, Stanford, CA 94305-4055

and

Peter W. Graves, Thomas J. Loretz and Raymond L. Roy

Detector Technology Inc.
P. O. Box K300, Brookfield, MA 01506

Abstract

High-gain microchannel plates (MCPs) which utilize curvature of the channel to inhibit ion feedback (C-plate MCPs) have demonstrated excellent performance characteristics. However, C-plate MCPs are at present costly to fabricate, and the shearing process used to curve the channels produces a low device yield. We describe here a totally new type of high-gain MCP structure in which each channel has an axially symmetric curvature. Initial tests of proof-of-concept units of these MCPs with 75-micron-diameter channels (macroplates) suggest that their performance characteristics have the potential to be equal to those of a C-plate MCP while the fabrication process is no more complex than that of a conventional straight-channel MCP.

Introduction

High-gain Microchannel Plates (MCPs) used to date have the configurations shown in Figure 1. "Chevron" and "Z-plate" MCP stacks, which are constructed from 2 or 3 MCPs having straight channels, are relatively easy to fabricate but do not have optimum performance characteristics. Even with bias angles of the order of 10 to 15 degrees, the trapping of positive ions at the interfaces of the plates is not completely effective, and there is a high level of residual ion feedback. In addition, spreading of charge at the interfaces degrades the spatial resolution of these MCP stacks when used with high-spatial-resolution readout systems. There is a further degradation of performance for high-resolution imaging systems caused by the broad pulse-height distributions of these MCPs at gain levels of the order of 10^6 to 10^7 electrons pulse^{-1}. The C-plate MCP, (Figure 1c), which employs curved channels to inhibit ion feedback in an identical manner to that used in a conventional channel electron multiplier (CEM), provides a high level of suppression of ion-feedback, a narrow output pulse-height distribution, and a very high spatial resolution. In particular, stable operation at gains in excess of 10^6 electrons pulse $^{-1}$, a resolution of the output pulse-height distribution of 30% or better, and a count rate capability in excess of 10^5 counts mm^{-2} s^{-1} have been realized with a single MCP with 12-micron-diameter channels on 15-micron centers.[1] Unfortunately, the shearing process required to introduce curvature into the channel is at this time difficult to control, the C-plates are at present costly to fabricate, and there is a low device yield.
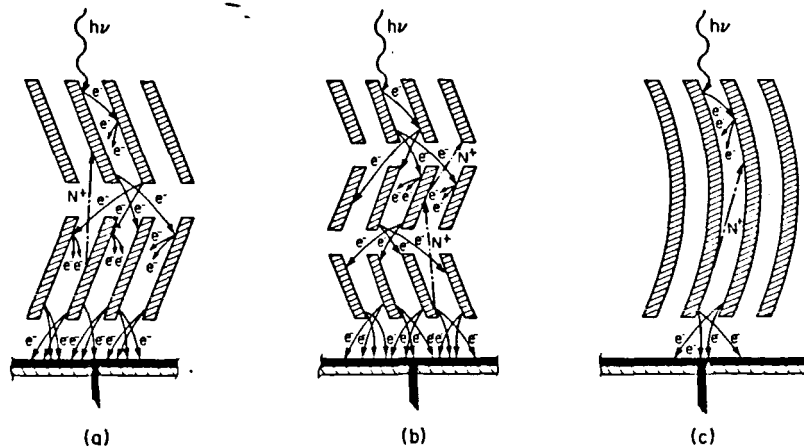
Figure 1. Configurations of high-gain MCPs.
a. "Chevron" MCP. b. "Z-plate" MCP. c. "C-plate" MCP.

In this paper we describe the performance characteristics of proof-of-concept units of an MCP structure which employs an axially symmetric twist of the channel to produce the curvature required to effectively inhibit ion feedback. Since the curvature is built into the channel at the time of the fiber draw, the "off-axis channel" MCP (patent pending) is as simple to fabricate as a conventional straight-channel MCP, yet has the potential to provide the superior performance characteristics of the sheared curved-channel MCP.

The "off-axis channel" macroplate

The configuration of the "off-axis channel" electron multiplier is shown in Figure 2. One or more channels are fabricated off-center within a larger glass fiber. Twisting the fiber produces a helical channel with the appropriate geometrical form to inhibit the trajectories of positive ions.
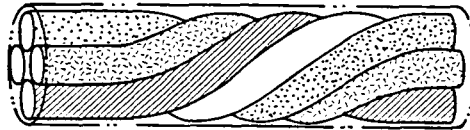
Figure 2. Configuration of the "off-axis channel" electron multiplier.

In order to produce a high-gain MCP with channels of this configuration, a number of requirements must be met. First, there must be about three or four channels per fiber in order to produce an open-area ratio equivalent to that of a conventional MCP. Second, for imaging applications, there must be an integral number of twists across the thickness of the plate in order to preserve the spatial relationship of the channel inputs and outputs. Third, in order to get at least one complete twist in a channel with a final diameter in the range from 10 to 25 microns, there must be a very high twist density in the original fiber.

As the first step in evaluating the "off-axis channel" concept, we have fabricated a number of 18-mm-format macroplates with active areas 15 mm in diameter and channel diameters of 75 microns. For ease of fabrication these proof-of-concept units employ only one channel per fiber, yielding a low open-area ratio of about 15%. Fibers of the type used to fabricate the macroplates are shown in Figure 3. Two macroplates have so far been tested, the first with a channel length-to-diameter ratio of 60:1, and the second with a channel length-to diameter ratio of 80:1.
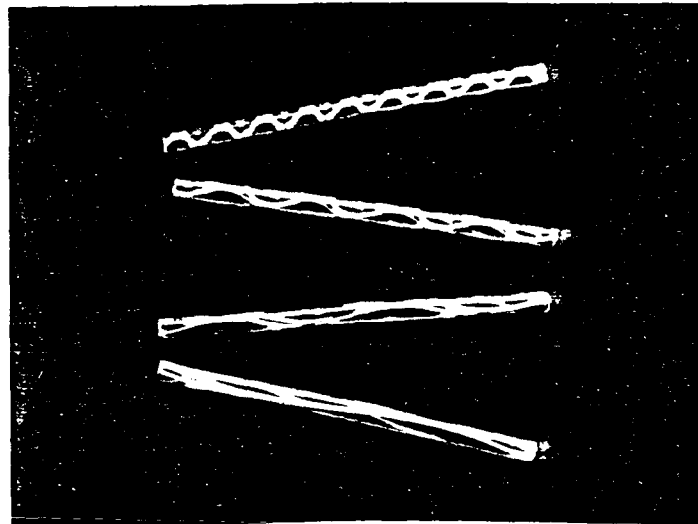
Figure 3. "Off-axis channel" fibers with different twist densities.

Performance Characteristics

Before evaluation both macroplates were subjected to bake and "scrub" procedures similar to those that we have developed for the C-plate MCPs.[1] However, because these macroplates employ channels of a totally new type, the evaluation program is being carried out in stages. For the initial tests, the first macroplate was baked in a hydrocarbon-free high-vacuum environment at a temperature of 120°C for a period of 24 hours and the second at 110°C for a period of 5 hours. Ultimately, the macroplates will be baked at 300° C until a pressure asymptote is attained. Each plate was "scrubbed" by operating it in a demountable MAMA detector tube[1] with the input face illuminated with ultraviolet photons from a mercury "penray" lamp. A total signal of 4×10^{10} counts, equivalent to a charge throughput of 0.01 C was accumulated before the initial evaluation. The resistances of the two macroplates were 25 MΩ and 31 MΩ respectively. In operation at an applied potential of 2400 V the strip current increased by about 12%, indicating that the temperature of the plate had increased by about 25 degrees C because of ohmic heating. However, no operating instabilities were observed.

The performance characteristics of both macroplates were very similar, with the exception that the resolution of the output pulse-height distribution (defined as $R = \Delta G/\bar{G}$ where ΔG = full width at half-height of the distribution and $\bar{G}$ = gain value at the peak of the saturated distribution) was somewhat superior for the plate with a channel length-to-diameter ratio of 80:1. Both macroplates demonstrated gain saturation at applied potentials in excess of 2000 V. The variations of the modal gain and the resolution of the output pulse-height distribution as functions of the applied potential are shown in Figure 4.
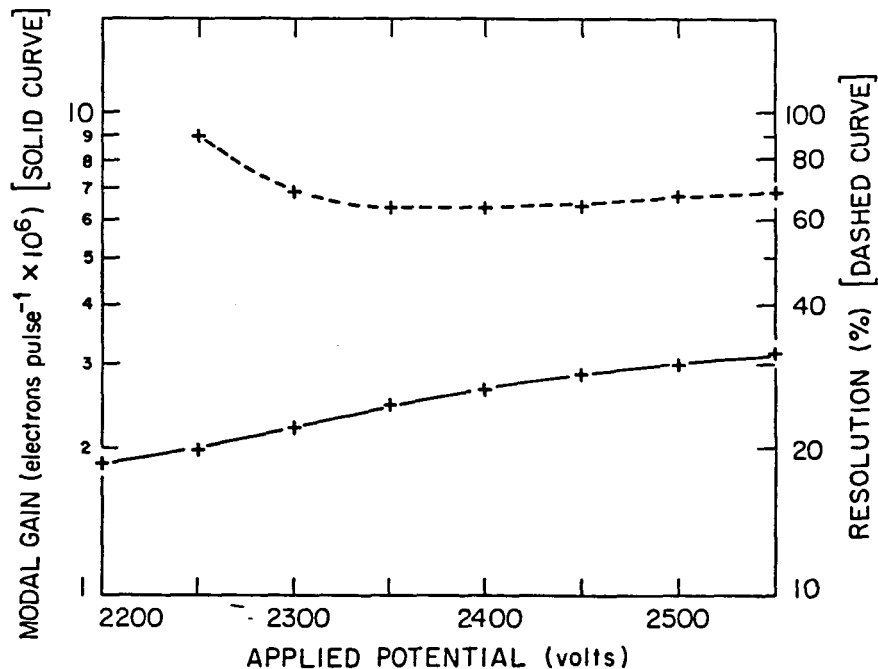
Figure 4. Variations of the modal gain and the resolution of the output pulse-height distribution as functions of the applied potential for the macroplate with an 80:1 channel length-to-diameter ratio. Macroplate was stimulated by 2537 A photons.

The saturated form of the output pulse-height distribution (see Figure 5) clearly demonstrates that the helical form of the channel is effective in suppressing ion feedback at high gain levels. The best resolution of the pulse-height distribution for the macroplate with a channel length-to-diameter ratio of 80:1 (~64%) is superior to the values that we have obtained in the past with "Chevron" and "Z-plate" MCP stacks.[2] The macroplate with a 60:1 channel length-to-diameter ratio yielded essentially identical gain values but the best resolution was about 71%. A further indication of the high level of suppression of ion feedback is the very low dark count rate (~0.3 counts s^{-1} for the total active area).
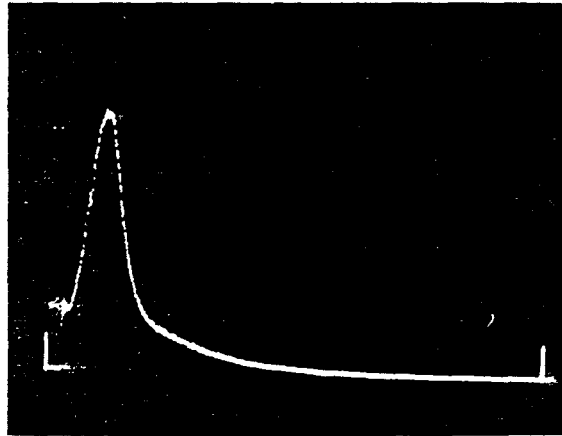
Figure 5.   Output pulse-height distribution for macroplate with 80:1
channel length-to-diameter ratio at an applied potential of 2400 V.
Modal gain 2.6×10^6 electrons pulse^{-1}, resolution 63.5%.

One immediate difference between the performance of the macroplate and   that of a
conventional MCP is the very strong dependence of the macroplate detection efficiency on
the electrostatic field strength at the input to the channels which is   caused by the low
open-area ratio. The macroplate was operated with the input face at a high negative
potential and the output face at ground.   By applying a higher negative potential on a
focusing electrode mounted in front of the macroplate, photoelectrons liberated on the
front-face electrode could be directed into the channels.   As shown in Figure 6, the
collection efficiency was a very sensitive function of the applied potential.   Further,
the focusing electrode potential for maximum detection efficiency varied with the distance
from the center of the macroplate.
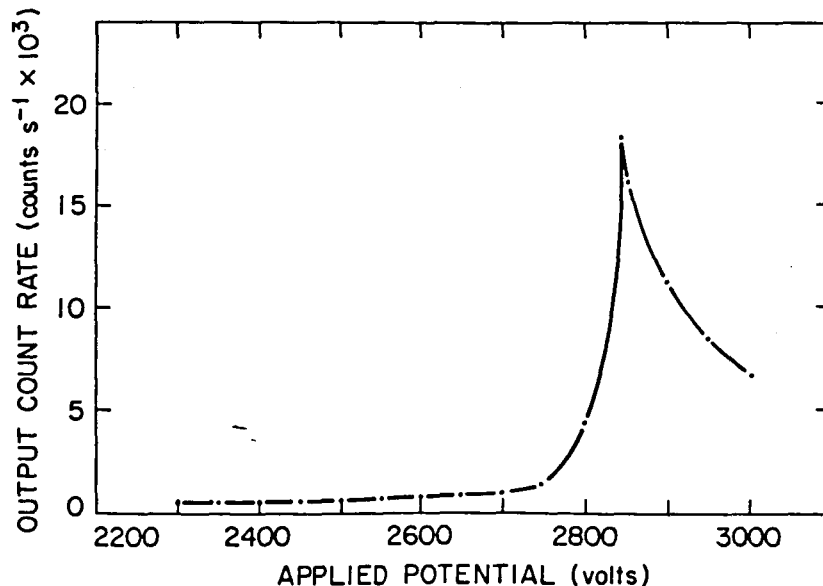
Figure 6.   Variation of the macroplate output count rate as a function
of the focusing electrode potential.   Macroplate input face potential
2400 V. Both electrodes operated at negative potentials with respect
to ground.   Center of macroplate illuminated with 2537 A photons.

Since the increase in the detection efficiency is significantly greater than the
closed-to-open area ratio, it is clear that there is a low detection efficiency within the
channels which is almost certainly caused by the combination of the zero bias angle of the
channels and the collimated input beam.   No significant gain changes were observed as a
function of the field electrode potential.   When the collection efficiency was optimized
by applying a suitable focusing electrode bias potential (typically in the range from 280
to 350 V negative of the macroplate input face potential), the variation of the output
count rate as a function of the macroplate potential had the form shown in Figure 7.
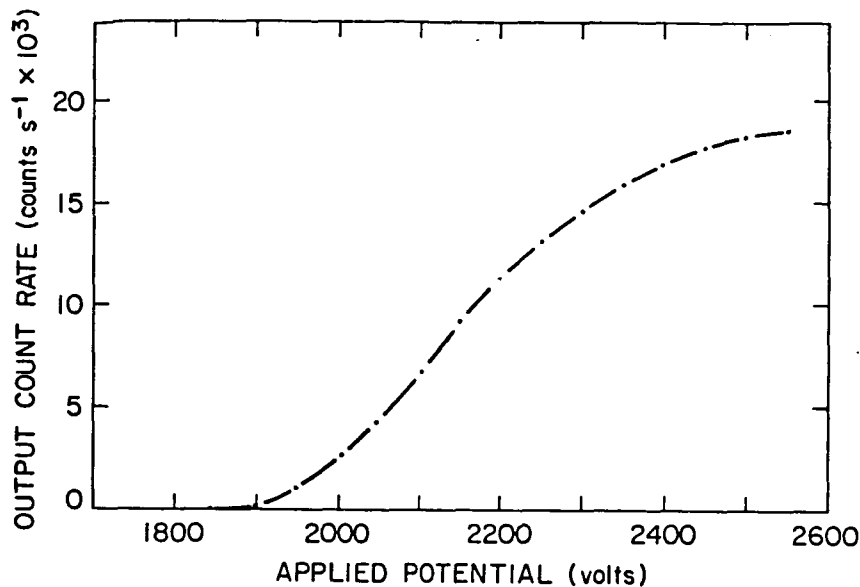
Figure 7. Variation of the output count rate as a function of the macroplate potential. Focusing electrode potential set for maximum detection efficiency. Center of macroplate illuminated with 2537 A photons.

The shape of this curve shows the characteristic plateau obtained with a high-gain channel multiplier providing a saturated output pulse-height distribution.

In summary, the data from the initial evaluations show clearly that the "off-axis channel" is effective in suppressing ion-feedback and that this structure can be used to construct a high-gain MCP.

Future Developments

With the "off-axis channel" concept validated, the need now is to demonstrate that this technology can produce a high-gain MCP with a channel diameter in the range from 10 to 25 microns and an open-area ratio of greater than 50%. The next step in the development program will be to produce sample MCPs with 25-micron channel diameters. The first units will again employ a single channel per fiber. Following this, the first MCPs with multiple channels per fiber will be fabricated, starting with large channel diameters and working down to diameters in the range from 10 to 25 microns. As soon as the first MCPs are available, imaging tests will be initiated to verify that the spatial relationship of the channel inputs and outputs can be maintained.

Acknowledgments

References

1. Timothy, J. G., "Curved-channel microchannel array plates," Rev. Sci. Instrum. 52, pp. 1131-1142. 1981.

2. Timothy, J. G., "Preliminary results with saturable microchannel array plates," Rev. Sci. Instrum. 45, pp. 834-837. 1974.

Imaging at Soft X-ray Wavelengths with High-Gain Microchannel Plate Detector Systems

J. Gethyn Timothy

Center for Space Science and Astrophysics,
ERL 313, Stanford University
Stanford, CA 94305 U.S.A. (415) 725-0444

Abstract

Multi-Anode Microchannel Array (MAMA) detector systems with formats of 256 x 1024 pixels and active areas of 6 x 26 mm^2 are now under evaluation at visible, ultraviolet and soft x-ray wavelengths. Very-large-format versions of the MAMA detectors with formats of 2048 x 2048 pixels and active areas of 52 x 52 mm^2 are under development for use in the NASA Goddard Space Flight Center's Space Telescope Imaging Spectrograph (STIS). Open-structure versions of these detectors with CsI photocathodes can provide a high-resolution imaging capability at extreme ultraviolet (EUV) and soft x-ray wavelengths and can deliver a maximum count rate from each array in excess of 10^6 counts s^{-1}. In addition, these detector systems have the unique capability to determine the arrival time of a detected photon to an accuracy of 100 ns or better. The construction, mode-of-operation and performance characteristics of the MAMA detectors are described and the program for the development of the very-large-format detectors is outlined.

Introduction

The Multi-Anode Microchannel Array (MAMA) detector systems are high-resolution pulse-counting images designed specifically for use in space. Laboratory and flight data have shown that the MAMAs provide the highest dynamic range and spatial resolution of any currently available pulse-counting imaging detector system.[1,2,3] Very-large-format MAMA detectors have been selected for use as the ultraviolet detectors in the NASA Goddard Space Flight Center's Space Telescope Imaging Spectrograph (STIS).[4] Open-structure versions of these detectors can be used as high-resolution imagers at extreme ultraviolet (EUV) and soft x-ray wavelengths and the basic technology used for the production of the STIS detectors can be further extended to produce ultra-large-format detectors with active areas of up to 140 mm in diameter. These detectors have many applications in the fields of high-energy astrophysics, laboratory plasma diagnostics and x-ray diffraction studies using synchrotron radiation. In this paper the construction, mode-of-operation and performance characteristics of the current generation of MAMA detectors are described. The program for the further optimization of the performance characteristics and for the fabrication of the very-large-format arrays is outlined.

Construction and Mode-of-Operation

In order to obtain the best possible spatial resolution and geometric fidelity and stability, the MAMA detector tube employs proximity-focused electron optics and does not require analog-interpolation or rise-time-discrimination techniques to locate the position of the detected photon event. As shown in the schematic in Fig. 1, the appropriate photocathode material is deposited on, or mounted in proximity focus with, the input face of a single high-gain curved-channel microchannel plate (MCP) electron multiplier. One of two photocathode configurations can be employed to produce a high detective quantum efficiency (DQE) at EUV and soft x-ray wavelengths, as shown in Fig. 2. The first is a high-density (opaque) CsI photocathode deposited directly on the front face of the MCP (Fig. 2a) and the second is a low-density (fluffy) CsI photocathode[5] mounted on a thin x-ray window in proximity focus with the input face of the MCP (Fig. 2b).

A photoelectron liberated from the photocathode is accelerated into the MCP channel and liberates secondary electrons at each impact with the semiconducting wall of the channel producing an electron gain of the order of 10^6. Curving the channel prevents the feedback of positive ions to the channel input where they can liberate secondary avalanches producing additional pulses which contribute to the background noise level and, in the limit, lead to unstable operation. The spatial location of the detected photon is determined by collecting the output charge cloud on a precision array of anode electrodes mounted in proximity focus with the output face of the MCP, the dimensions of the electrodes being smaller than the dimensions of the defined pixel. Coincident detection of the charge cloud on two or more electrodes permits a very large number of pixels to be defined while requiring only a relatively small number of amplifier and discriminator circuits.